Geoelectrical monitoring of embankment dams for detection of internal erosion - work in progress in Sweden

R. Norooz
Engineering Geology, Lund University, Lund, Sweden & Sweco Sverige AB, Malmö, Sweden
T. Dahlin
Engineering Geology, Lund University, Lund, Sweden
P.I. Olsson
Engineering Geology, Lund University, Lund, Sweden & WSP Sverige AB, Malmö, Sweden
A. Nivorlis
Engineering Geology, Lund University, Lund, Sweden
T. Günther
Leibniz Institute of Applied Geophysics, Hannover, Germany
C. Bernstone
Vattenfall AB, Solna, Sweden

ABSTRACT: The demand for better methods for condition control and monitoring of embankment dams is increasing because of their increasing age and higher demands on availability. One major risk threatening embankment dam integrity is internal erosion of the core. Internal erosion often progresses inside the dam structure, but it is difficult to detect with conventional methods. Electrical resistivity tomography (ERT) can be used to monitor the interior of the dam as a complementary monitoring method, to detect internal erosion and flow-induced variation in the resistivity values caused by the temperature and TDS, and grain size changes. In Sweden the electrodes are generally installed along the dam crest, in the top of the core, using a 2D ERT approach. This has the advantage of focusing the sensitivity to the core itself, which is the most critical part for internal erosion. However, the orientation of the electrode layout in combination with the 2D approximation leads to severe 3D effects, which distorts the inverted model resistivities and geometry. This study was carried out using a new approach wherein the 3D geometry of the dam and the internal zonation were incorporated in the inversion modelling of the collected ERT data from a test embankment dam. The test dam with a height of 4 m, containing some intentional artificial defects in the core and fine filter, was constructed in Älvkarleby, Sweden with the purpose of assessing different monitoring techniques including ERT. Electrodes installed inside the embankment, on top of the core and in the upstream and downstream filters, were used to acquire around 7000 to 14,000 data points on a daily basis for over 2 years. The inversion models successfully located 2 out of 5 defects in the core, a horizontal and a verical crushed rock zone, with a slight location shift for the horizontal zone. The concrete block was indicated, although not as distinctly and with a lateral shift. The crushed rock zone at the abutment and the wooden box could not be discovered, and the defect placed inside the fine filter was not detected. Several unintentional anomalous zones were also detected.

1 INTRODUCTION

Demands for the availability of the hydropower system are increasing since generating electricity from wind and solar power is growing, in combination with phasing out nuclear reactors and fossil fuel power. Large repair and/or reconstruction measures are time-consuming and lead to a lack of availability. Effective monitoring systems support the robustness of the energy system, as they can assist in detecting defects at an early stage and make it possible to plan maintenance and repair and it can affect the availability. This, in turn, makes it possible to continue to use hydropower as efficient regulating power. Maintaining the existing hydropower infrastructure means resource efficiency, which is essential for a stable future electrical power supply.

Most of the Swedish dams were built during the great development of hydropower in Sweden during the 20th century, with peaks in investment 50 and 100 years ago (Swedish power association, 1981). The average age of Swedish embankment dams is today about 60 years (Bernstone, 2006). Degrading processes can give rise to increasing seepage of water through the core of the dam, which can lead to the transport of soil particles, thus creating internal erosion in embankment dams. Internal erosion is one of the main causes of embankment dam failure together with overtopping. If internal erosion remains undetected, it may lead to dam failure. Internal defects are however difficult to detect as they are invisible from the surface, and the early-stage detection capability of present instrumentation systems can be improved.

ERT has been tested as a complementary method for continuous monitoring in embankment dams with promising results. Time-lapse ERT measurements can provide spatial coverage of the interior of the embankment over time, where changes and anomalous seasonal variation in resistivity can provide insights about internal problem zones. A major advantage of ERT includes the ability to provide information on the interior of a dam in an essentially non-destructive way at a reasonable investment.

A number of studies have been conducted using geophysical methods as a monitoring system to detect leakage and analyze the stability of embankment dams (e.g., Yaya et al. 2017; Lee et al. 2020). Sjödahl et al. (2008) used resistivity monitoring data to discover leakage and internal erosion in Hällby embankment dam. This dam was the first Swedish dam where electrical resistivity equipment was installed permanently as a monitoring system. The results showed increasing long-term resistivity variations in the left abutment relative to other parts. It might be related to the ongoing internal erosion process in the dam. Sjödahl et al. (2009) also evaluated seepage in Sädva dam using time-lapse ERT. It was concluded that time-lapse ERT measurements could be used to assess the seepage through the dam qualitatively. There were no indications of safety problems in Sädva dam; however, some parts with high resistivity variations should be kept under observation. These methods are based on the seasonal temperature and total dissolved solid changes in the water reservoir. These variations propagate through seepage and soil resistivity is also affected. Time-lapse ERT could measure these changes and track the seepage path.

Some researchers used ERT in combination with other methods to detect leakage (e.g., Dai et al. 2017; Martínez-Moreno et al. 2018). Guo et al. (2022) used self-potential (SP) and ERT to discover seepage paths in an earth-filled dam which already has some signs of erosion. Three seepage paths based on the negative anomaly of SP and the low resistivity of ERT consistent with the six seepage outfalls were detected.

Some researchers used lab models and test dams to detect the capability of ERT in detecting leakage (e.g., Shin et al. 2019; Masi et al. 2019). Hojat et al. (2021) used ERT and Fiber Optic Techniques to detect seepage zones in a test embankment. The results showed that ERT measurements could discover seepage and fibre optic sensors showed the seepage with a short delay compared to ERT.

Short-term time-lapse 2D ERT measurements to investigate weak zones in Røssvatn test embankment dam were used (Sjödahl, 2010). The results showed that time-lapse ERT measurements in connection with changes in the reservoir level are useful for discovering leakage paths, which was confirmed but short-term monitoring on a small embankment dam (Sjödahl, 2011).

In embankment dams, effects from the disregarded (third) dimension effects caused by the slopes and internal regions distort the ERT data, and the assumptions of infinitely extended structures perpendicular to the electrode layout in the calculation of geometric factors are no longer accurate. Thus, it is necessary to consider the distortions and the induced errors in inverse modelling. Hence, researchers used different techniques such as 3D calculations of the geometric factors and 3D inversion models to consider the distortions due to 3D effects. Bièvre et al. (2018)

used 3D computation of geometric factors in a 2D inversion model and could improve the interpretation of 2D ERT data collected from a dyke. These techniques for compensation for the 3D character of the surface geometry, would however not work for handling the 3D effects caused by the internal zonation of typical Swedish embankment dams. Norooz et al. (2021) developed a 3D ERT inverse model as a pre-study for ERT measurements in Älvkarleby test embankment dam in Sweden. They used priori information about the resistivity of different zones of the test dam in the inversion model. The proposed methodology, given that priori information is available, could decrease non-uniqueness in the inversion and increase the effectiveness of ERT time-lapse monitoring. The mentioned 3D effects on ERT data need to be further studied and a methodology with an inverse model considering the 3D context of embankment dams is required.

The purpose of this study is to assess the capability of ERT measurements as a monitoring tool for internal erosion detection in embankment dams applying inverse modelling considering the 3D character of embankment dams. A test embankment dam with a height of 4 m, containing some simulated defects in the core and fine filter, was constructed in Älvkarleby with the purpose of assessing different monitoring techniques including ERT. This study was carried out within that framework, whereas a new approach, the 3D geometry of the dam, the internal zonation and the 3D calculation of the geometric factor were incorporated in the inversion modelling.

2 MATERIAL AND METHODS

2.1 *Älvkarleby test embankment dam*

Vattenfall has built a pilot-scale embankment dam in Älvkarleby to assess the damage detection capability of several dam monitoring methods, including ERT. The dam was built as a conventional zoned embankment dam, in a concrete container with an inner dimension of 20 m * 16 m * 4 m (Fig. 1). The dam core is 1.6 m wide at the base which reduces to 1.1 m at the top, and reaches to 0.5 m below the crest of the dam. The core is overlain by 0.1 m fine filter material and 0.4 m structural fill material. The fine filter is 0.9 m wide and the coarse filter 0.1 m wide (Bernstone et al. 2021).

Several small defects were intentionally placed inside the core and fine filter, as indicated by the red rectangles in Figure 2. The shape, size and positions of the defects are shown in Table 1.

2.2 *ERT set-up at the Älvkarleby test embankment dam*

In total 224 electrodes were installed for ERT in the test embankment, where Figure 3 shows the 3D placement of the electrode spreads. Six horizontal buried electrode lines with around 61 cm electrode spacing were used: on top of the clayey till core and at two levels in the filters adjacent to the core, bottom and middle. In addition, four vertical electrode lines were used with 50 cm vertical spacing at each end in the filter of the dam. There are 32 electrodes in each horizontal layout, and 8 electrodes in the slightly inclined vertical layouts at the ends.

A permanent monitoring system capable of measuring ERT was installed at the test site, which is connected to electrode cables and electrodes that are embedded in the embankment dam. Stainless steel plates are used as electrodes. An ABEM Terrameter LS2 is used for the measurements, which is connected to a relay switch that connects different 2 x 32 electrode combinations to the instrument so that the different layout combinations can be accessed sequentially.

Different types of configurations including bipole-bipole (Zhou & Greenhalg, 2000), extended gradient (Zhou et al. 2020), multiple gradient (Dahlin & Zhou, 2006) and corner (Tejero-Andrade et al. 2015) arrays were used in the ERT measurements. The measurement profiles were designed in a way to provide sufficient data points which can cover the whole core volume and increase the defect detection capability while at the same time adhering to the zoned construction of the dam. Initially, around 7000 ERT data points were collected on a daily basis, which was increased in a couple of steps to be around 14,000 in the later part of the monitoring by adding non-standard and asymmetric electrode combinations. Hence the size of the data sets used in the inverse modelling has increased accordingly.

Figure 1. Aerial view of Älvkarleby test dam (Bernstone et al. 2021)

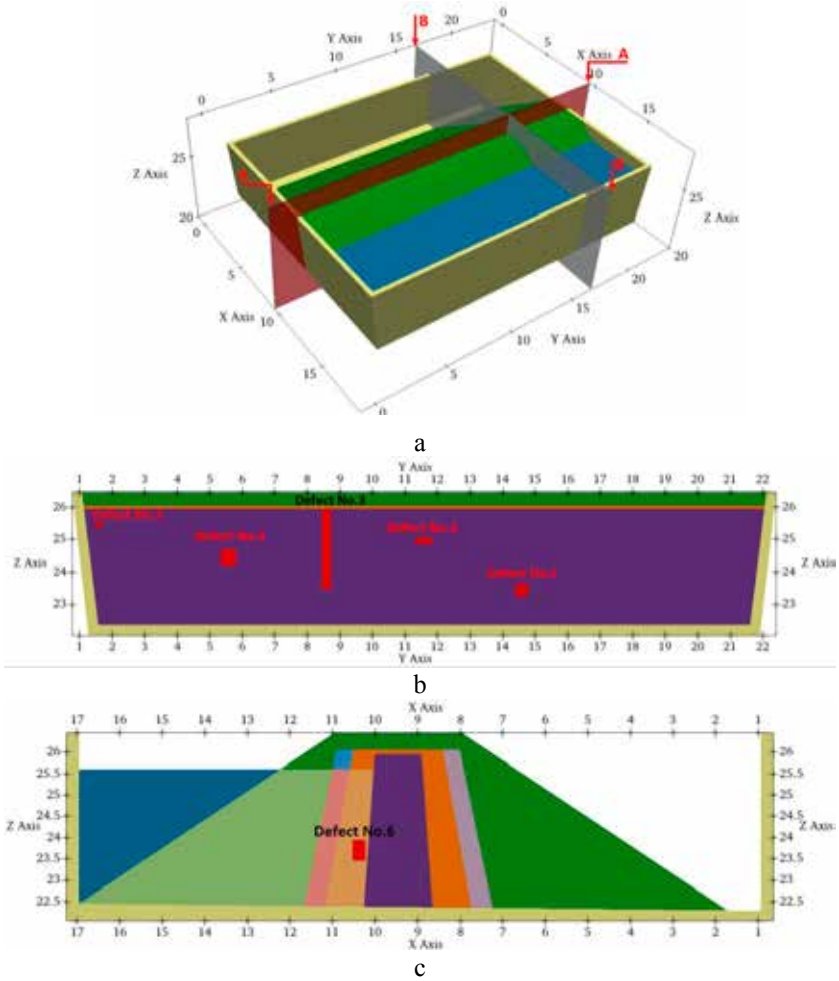

a

b

c

Figure 2. a) Location of the cross-section planes and 3d view of the dam; b) Section A and the position of defects in the core; c) Section B and the position of the defect in the filter.

Table 1. Defects placed in the clay core and fine filter (Lagerlund et al. 2022)

No.	Type	Material	Shape	Size (m)
1	Cavity	Wood	Cube	0.4 x 0.4 x 0.4
2	Horizontal permeable zone centrally	Crushed rock, 4-8 mm	Cuboid	0.5 x 0.1
3	Vertical loose zone	Crushed rock, 8-64 mm	Cylinder	0.3
4	Boulder	Concrete cube	Cube	0.5 x 0.5 x 0.5
5	Horizontal permeable zone - at the abutment	Crushed rock, 4-8 mm	Cuboid	0.2 x 0.2
6	Fine filter defect on the upstream side	Crushed rock, 8-64 mm	Cuboid	0.3 x 0.3

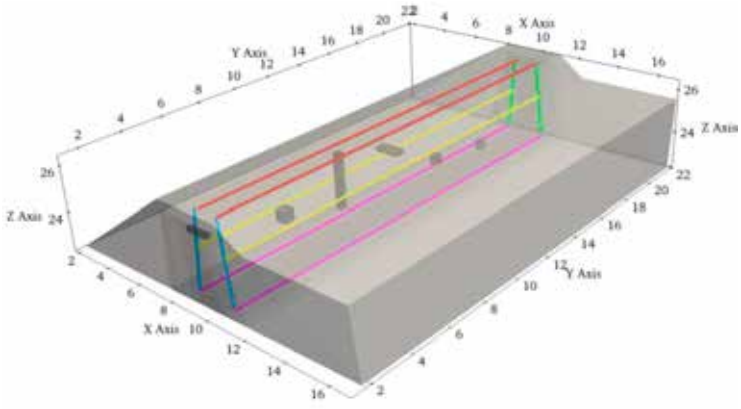

Figure 3. Position of measurement lines.

2.3 *Inversion modelling*

The pyBERT/pyGIMLi software package was used for the inverse numerical modelling (Rücker et al. 2017). In this research, 3D time-lapse inversion model with 3D geometric factor calculations was used. The mesh used for the inversion calculations consists of a number of around 200,000 cells (Fig. 4), distributed between 12 regions with broken smoothness constraints between them (Figs. 5). The regions are based on the zoned construction material distribution of the dam in combination with the water saturation status of the material zones, and the mesh was generated using the TetGen software and iteratively controlled by the user until the final appropriate mesh was reached (Si, 2015).

For all models robust (L1) methods were applied, in order to avoid smooth transitions and consider the sharp transitions between the dam zonations in the inverse modelling. A Lambda value of 40 and a noise of 0.5% were used. The Jacobian matrix was recalculated in each iteration. In the time-lapse model, a reference model-based scheme which applies a full minimization in each time-step of data while the model is constrained to the first data set was used. In the study by Norooz et al. (2021), the resistivity values of each dam zone were used as the prior information in the inversion model, but not used for the inversion here.

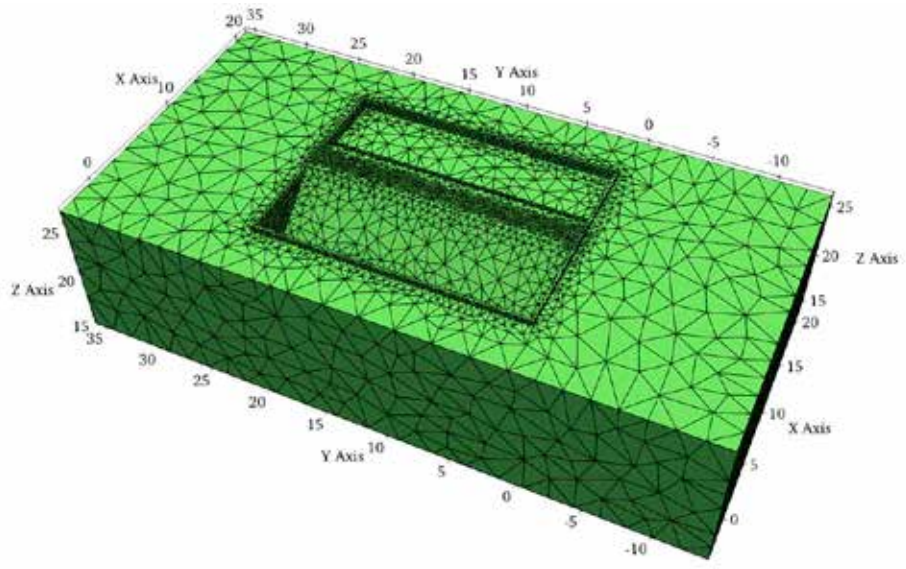

Figure 4. The generated mesh for the inversion model.

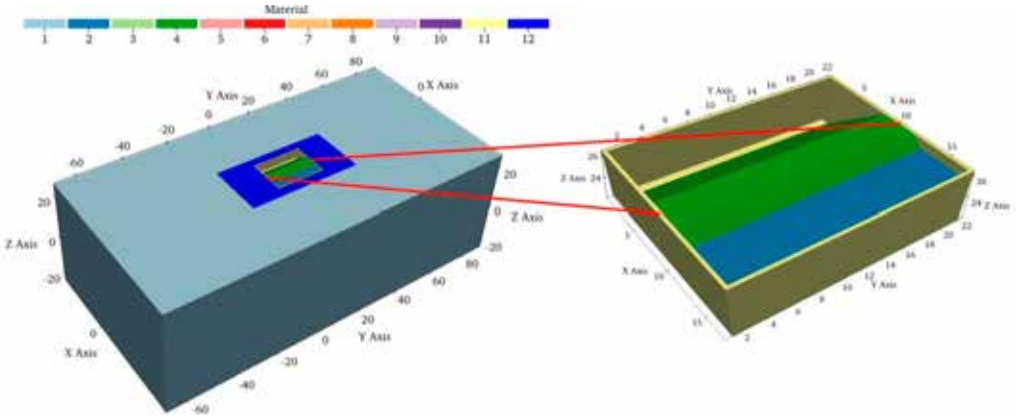

Figure 5. Simulated regions in the geometry used in the inversion model.

Some synthetic data sets using pyBERT/pyGIMLi were generated. In the model, several small defects with higher resistivity were placed inside the core since zones affected by internal erosion are expected to have higher resistivity values in comparison to the surrounding core material as in the encoded areas the fine materials are washed out and the coarse materials with higher resistivity are left. The defects are larger than the real defects since TetGen software was not able to generate a mesh that can handle a model with smaller defects. The synthetic data were inverted with the same settings as used in the inverse modeling of the field ERT data. The analyses of synthetic ERT data could detect the location of the simulated defects with areas with higher resistivity values (Fig. 6).

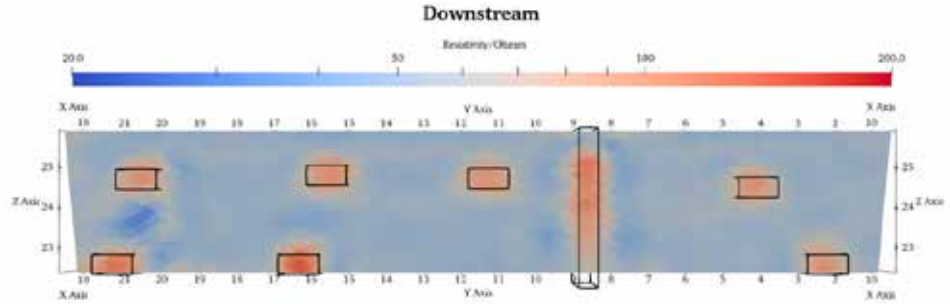

Figure 6. The inversion results of the synthetic ERT data in the core (the location of the simulated defects is shown by black cuboids).

3 INVERSION RESULTS OF FIELD DATA

In all of the timeframes of the inversion model, the error level was less than 2 percent. In the following, the results of inverse modeling in the core of the dam are presented. This means that other parts of the dam body have been cut from around the core so that it is easier to see the results in the dam core where the defects are located (Fig. 7).

The results of two sets of inversion models, one containing data from around 100 days in the period 2019-12-12 to 2022-01-28 and one containing data from around 20 days from 2021-08-27 to 2022-01-21 are presented in the following.

From 2019-12-12 to 2022-01-28, the water level was fluctuating whereas from 2021-08-27 to 2022-01-21, the water level was decreasing and then was constant up to the end of the period (Fig. 8 a, b). The data sets for the inversion models were chosen in a way to consider the effects of water fluctuation in the ERT data. The water level in the reservoir could affect the measured resistivity and it helped to assess whether the inversion models are predicting the resistivity values properly based on the changes in the reservoir. As well as the defect zones are more sensitive to the reservoir level changes which lead to more changes in resistivity and make it easier for time-lapse ERT data to detect them.

In both of the inversion models, the first data sets (data set 2019-12-12 and data set 2021-08-27) were chosen as the reference model. The following analyses focus on the average of the inverted resistivity values (Fig. 9).

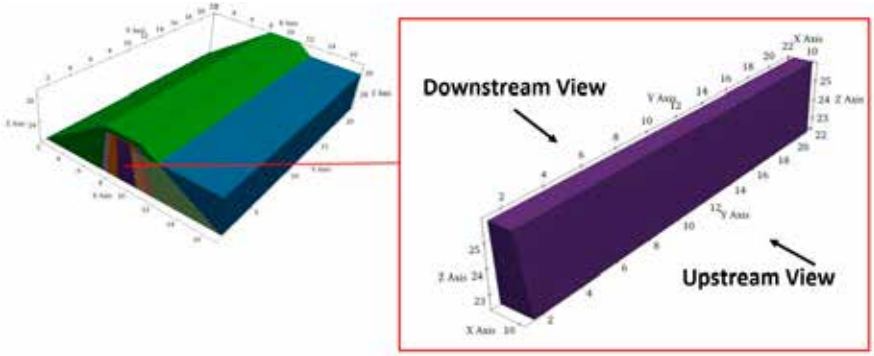

Figure 7. The upstream and downstream view of the uncovered core.

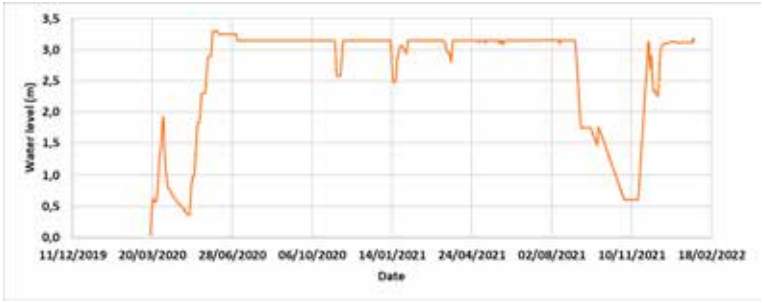

a

b

Figure 8. a) The water level in the reservoir from 2019-12-12 to 2022-01-28; b) The water level in the reservoir from 2021-08-27 to 2022-01-21.

The simulated cavity which is named Defect No. 1 (see Table 1) was not detected (Fig. 9 a, b). In addition to the relative small size of the defect, water absorption by the wood can have made the resistivity contrast relative to the surrounding core material small, where water-saturated wood may have a resistivity significantly less than 100 Ωm (Fediuk et al. 2020; Martin 2012).

The horizontal crushed rock zone (Defect No. 2 in Table 1) which simulates a permeable area was discovered by both of the inversion models; the one containing data sets from 2019-12-12 to 2022-01-28 (Fig. 9 a) and the other one containing data sets from 2021-08-27 to 2022-01-21 (Fig. 9 b). However, it is detected with some distance from the real location which is indicated by the

full-drawn line box in Figure 9. The predicted location of the defect is shown by the dotted line bounding box in Figure 9 where the dotted line bounding box is placed at the center of the area with the high resistivity. The crushed rock material has higher resistivity values than the core material and it made it easy for ERT to detect it.

The vertical crushed rock zone which is named Defect No. 3 (see Table 1) was detected as the vertical high resistivity area by both model analysis approaches (Fig. 9 a, b).

There are some high resistivity areas around the concrete cube (Defect No. 4 in Table 1) in Figure 9 a which is difficult to interpret as the location of Defect No. 4. In Figure 9 a, dotted line bounding boxes at the center of the areas with high resistivity are placed. There are no areas with anomalous resistivity around Defect No. 4 in Figure 9 b, in contrast to the average inverse model in Figure 9 a.

The small crushed rock zone near the abutment (Defect No. 5 in Table 1) was not detected at all (Fig. 9 a, b). Reasons that contribute to this are related to the small size, the proximity of the concrete wall and the low coverage of the data near the abutments.

Other areas than the simulated defects with high resistivity values (the yellow bounding boxes in Fig. 9) were discovered which could possibly be related to buried sensors and cables for other methods, or unintentional variation in material properties, temperature or water content, that might be associated with prefential flow paths. Another possible partial explanation could be inversion artefacts, but the synthetic modelling results suggest that this is not the case.

The inversion model containing the data sets from 2019-12-12 to 2022-01-28 was more successful in detecting the location of the defects (Fig. 9 a). It could partly discover Defect No. 4 as well as Defect No. 2 with less distance from the real location while the model containing the data sets from 2021-08-27 to 2022-01-21 (Fig. 9 b) could not discover Defect No. 4 and Defect No. 2 was discovered with more distance from the real location.

The ERT measurements were not able to detect the defect in the filter which might be related to the low data coverage in the filter and limited resistivity contrast between the filter defect and filter material.

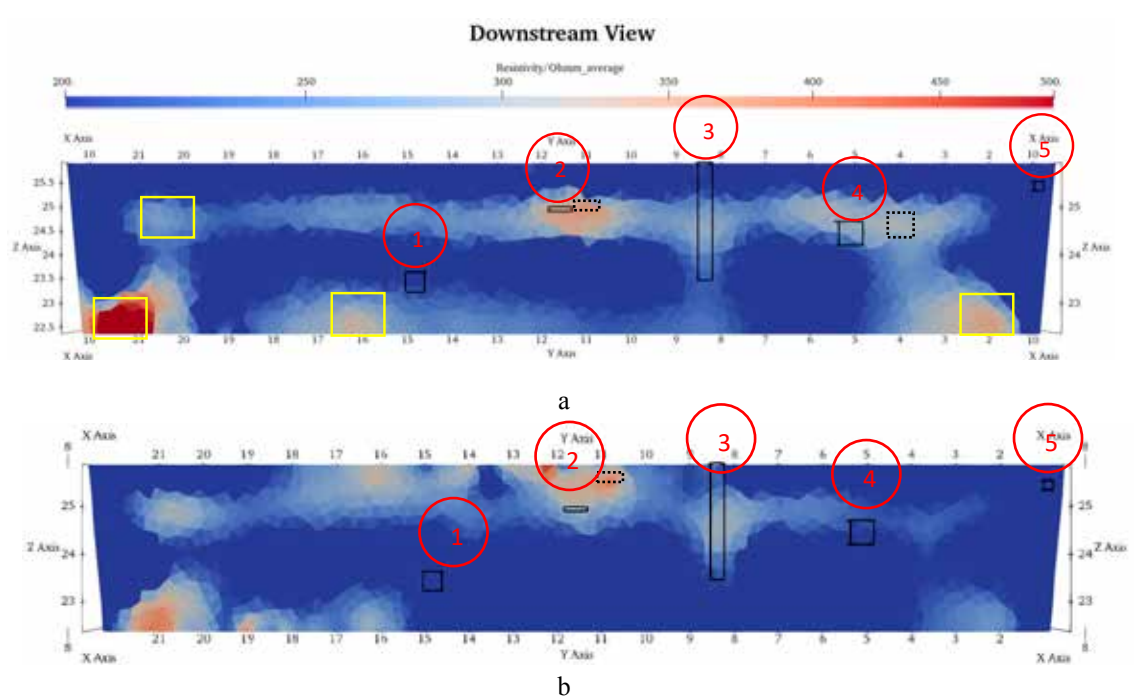

Figure 9. a) The average value of the inverted field ERT data through the whole period (from 2019-12-12 to 2022-01-28); b) The average value of the inverted field ERT data through the period from 2021-08-27 to 2022-01-21; The location of the defects is shown by full-drawn black cuboids, whereas the predicted location is indicated by dotted lines.

4 CONCLUSIONS

ERT measurements in the test embankment dam were successful in discovering 2 out of 5 intentionally built-in defects. These defects, a horizontal and a vertical crushed rock zones, were associated with a higher resistivity contrast. So ERT has the potential to detect the eroded zones in typical Swedish dams which usually have higher resistivity values in comparison to the healthy surrounding core material. Furthermore, the concrete cube was indicated but not as distinctly, probably due to less resistivity contrast between the wetted concrete and the core material. The two other core defects, the wooden box and another horizontal crushed rock zone at the abutment, were not detected which could be related to the low resistivity contrast with the surrounding material, the small size of the defects, the position immediately next to a material transition or low data coverage.

The ERT measurements were not also able to detect the defect in the filter which might be related to the low coverage of data in the filter and the limited resistivity contrast between the filter defect and filter material.

The time-lapse inversion results showed that ERT was not able to predict the size of the defects but it obtained some hints about the relative location and shape of the defects which is valuable.

Additional anomalous zones than the defects were discovered which could possibly be related to buried sensors and cables for other methods, or unintentional variation in material properties, temperature or water content, that might be associated with prefential flow paths.

The tests presented here cannot be used to fully evaluate the capability of ERT monitoring to detect internal erosion under typical Swedish conditions, because the permeable defects that go through the core do not lead to any significant flow of water that would be associated with a seasonal variation in resistivity. This is caused by hydraulically tight fine filters on either side of the core in combination with the small hydraulic gradient that follows with the shallow position of the defects. On the other hand, the electrode density in the test dam installations is high in relation to what might be achieved on existing dams, so further research is needed for the evaluation of what can be achieved in actual dams.

5 ACKNOWLEDGEMENTS

The research presented here was funded by Swedish Energy Agency (project 48411-1), Swedish Centre for Sustainable Hydropower- SVC (project VKU14177) and Vattenfall AB. SVC has been established by the Swedish Energy Agency, Energiforsk and Svenska Kraftnät together with Luleå University of Technology, KTH Royal Institute of Technology, Chalmers University of Technology, Uppsala University and Lund University (http://www.svc.nu).

The computations were performed on resources provided by the Swedish National Infrastructure for Computing (SNIC) at LUNARC. We wish to thank our colleagues at LUNARC for their valuable support in connection with the study.

We are also grateful to Karl Butler and Léa Lévy for a series of constructive discussions on data processing, inversion and interpretation, which resulted from Karl's visit in Lund that was supported by a guest researcher grant from the Wenner-Gren Foundation (GFOv2020-0008).

6 REFERENCES

Bernstone, C. 2006. *Automated performance monitoring of concrete dams*, PhD thesis, Lund University, ISBN 91-628-6982-5, 201p.

Bièvre, G. Oxarango, L. Günther, T. Goutaland, D. & Massardi, M. 2018. Improvement of 2D ERT measurements conducted along a small earth-filled dyke using 3D topographic data and 3D computation of geometric factors. *Journal of Applied Geophysics* 153: 100-112.

Dahlin, T. & Zhou, B. 2006. Gradient array measurements for multichannel 2D resistivity imaging. *Near Surface Geophysics* 4 (2): 113 – 123.

Dai, Q. Lina, F. Wang, X. Fenga, D. & Bayless, R.C. 2017. Detection of concrete dam leakage using an integrated geophysical technique based on flow-field fitting method. *Journal of Applied Geophysics*. Vol. 140. pp. 168–176.

Fediuk A., Wilken D., Wunderlich T. & Rabbel W. 2020. Physical Parameters and Contrasts of Wooden Objects in Lacustrine Environment: Ground Penetrating Radar and Geoelectrics. *Geosciences* 10, 146.

Guo, Y. Yian, C. Xie, J. Luo, Y. Zhang, P. Liu, H. & Liu, J. 2022. Seepage detection in earth-filled dam from self-potential and electrical resistivity tomography. *Engineering Geology* 306.

Hojat, A. Ferrario, M. Arosio, D. Brunero, M. Ivanov, V.I. Longoni, L. Madaschi, A. Papini, M. Tresoldi G. & Zanzi, L. 2021. Laboratory Studies Using Electrical Resistivity Tomography and Fiber Optic Techniques to Detect Seepage Zones in River Embankments. *Geosciences* 11: 69.

Lagerlund, J. Bernstone, C. Viklander, P. & Nordström, E. 2022. *Embankment Test Dam of Älvkarleby - Description of installed defects and their position*. Mendeley Data. V3.

Bernstone, C. Lagerlund, J. Toromanovic, J. & Juhlin, C. 2021. *Deformationer och portryck i en experimentell fyllningsdamm*, Energiforsk report.

Lee, B. Oh, S. & Yi, M.J. 2020. Mapping of leakage paths in damaged embankment using modified resistivity array method. *Engineering Geology* 266: 5.

Martin T. 2012. Complex resistivity measurements on oak. *European Journal of Wood and Wood Products*. 70, 45–53

Martínez-Moreno, F.J. Delgado-Ramos, F. Galindo-Zaldivar, J. Martín-Rosales, W. López-Chicano, M. & González-Castillo, L. 2018. Identification of leakage and potential areas for internal erosion combining ERT and IP techniques at the Negratín Dam left abutment (Granada, southern Spain), *Engineering Geology*. Vol. 240. pp. 74-80.

Masi, M. Ferdos, F. Losito, G. & Solari, L. 2020. Monitoring of internal erosion processes by time-lapse electrical resistivity tomography. *Journal of Hydrology* 589.

Norooz, R. Olsson, P.I. Dahlin, T. Günther, T. & Bernstone, C. 2021. A geoelectrical pre-study of Älvkarleby test embankment dam: 3D forward modelling and effects of structural constraints on the 3D inversion model of zoned embankment dams. *Journal of Applied Geophysics* 191.

Rücker, C. Günther, T.T. & Wagner, F.M. 2017. pyGIMLi: An open-source library for modelling and inversion in geophysics. *Computers and Geosciences* 109: 106-123.

Shin, S. Park, S. & Kim, J.H. 2019. Time-lapse electrical resistivity tomography characterization for piping detection in earthen dam model of a sandbox. *Journal of Applied Geophysics* 170.

Si, H. 2015. TetGen. a Delaunay-Based Quality Tetrahedral Mesh Generator: ACM Transactions on Mathematical Software (TOMS) 41.

Sjödahl, P. Dahlin, T. Johansson, S. & Loke, M.H. 2008. Resistivity monitoring for leakage and internal erosion detection at Hällby embankment dam. *Journal of Applied Geophysics*. Vol. 65. pp. 155–164.

Sjödahl, P. Dahlin, T. & Johansson, S. 2009. Estimating seepage flow from resistivity monitoring data at the Sädva embankment dam. *Near Surface Geophysics*. Vol. 7. pp. 463-474.

Sjödahl, P. Dahlin, T. & Johansson, S. 2010. Using the electrical resistivity method for leakage detection in a blind test at the Røssvatn embankment dam test facility in Norway. *Bulletin of Engineering Geology and the Environment*. Vol. 69. pp. 643–658.

Sjödahl, P. Johansson, S. & Dahlin, T. 2011. Investigation of shallow leakage zones in a small embankment dam using repeated resistivity measurements in Internal erosion in embankment dams and their foundations, ed. J-J Fry, J Riha, T Julinek, ISBN 978-80-7204-736-9, *Proceedings of the Institute of Water Structures FCE BUT Brno*, Volume 13. 26-29 April 2011. Brno. Czech Republic. pp. 165-172.

Swedish Power Association. 1981. *Hydropower in Sweden*, ISBN 91-7186-064-9. 143p.

Tejero-Andrade, A. Cifuentes, G. Chávez, R.E. López-González, A.E. & Delgado-Solórzano, C. 2015. L- and CORNER-arrays for 3D electric resistivity tomography: an alternative for geophysical surveys in urban zones. *Near Surface Geophysics* 13: 355-367.

Yaya, C. Tikou, B. & LiZhen, C. 2017. Numerical analysis and geophysical monitoring for stability assessment of the Northwest tailings dam at Westwood Mine, *International Journal of Mining Science and* Technology. Vol. 27. No. 4.

Zhou, B. Bouzidi, Y. Ullah, S. & Asim, M. 2020. A full-range gradient survey for 2D electrical resistivity tomography. *Near Surface Geophysics*. 18 (6): 609-626.

Zhou, B. & Greenhalg, A.A. 2000. Cross-hole resistivity tomography using different electrode configurations. *Geophysics Prospect* 48:887-912.